Improved Boost Converter with Functions of Adjustable Output Voltages and Currents

Cheng-Tao Tsai[*] and Feng-Wei Peng

Department of Electrical Engineering, National Chin-Yi University of Technology, Taichung 41170, Taiwan

In this paper, we propose an improved boost converter with functions of adjustable output voltages and currents. The DC sources of electronic products using batteries have become indispensable equipment. These charging sources of the diverse batteries must be provided by switching power converters. To obtain functions of adjustable output voltages and currents, a conventional boost converter is usually accepted. However, the power semiconductor devices (power switches and power diodes) of the conventional boost converter are operated at high frequency, which causes high power losses, high temperatures, and low conversion efficiency. To overcome these disadvantages, a passive lossless snubber is incorporated in the conventional boost converter to reduce power losses and increase conversion efficiency. In this paper, we propose an improved boost converter to implement functions of adjustable output voltages and currents. We compare the performance and efficiency between the conventional and improved boost converter with functions of adjustable output voltages and currents. Theoretical analysis and experimental results confirmed that the improved boost converters with functions of adjustable output voltages and currents has lower power losses, lower temperatures and higher conversion efficiency than the conventional boost converter.

1. Introduction

The progress and development of electronic products make people's life more convenient and comfortable. Most electronic products need batteries to provide power, such as LEDs, cell phones, uninterruptible power systems (UPS), and electric vehicles. These electronic products using voltages of batteries are also becoming more and more diverse. For example, 12, 24, 36, and 48 V_{DC} sources of batteries are required.[1–3] These charging sources of the diverse batteries must be provided by power converters.

A conventional boost converter that uses pulse width modulated techniques is operated at high frequency to control power semiconductor devices. The objective of high–frequency operation in the conventional boost converter is to increase conversion power and reduce component size. However, increasing the switching frequency results in high temperatures, high power losses, and low conversion efficiency in power semiconductor devices.[4–6] High power

---

losses are generally caused by non-ideal parasitic elements of semiconductor devices operated at high-frequency turned-on and turned-off switching transitions. Thus, the reduction of switching losses becomes an important design issue. Conventional snubbers combined with passive components (diodes, capacitors, and resistors) to decrease the high temperatures and power losses of power semiconductor devices are usually adopted. However, these passive snubbers dissipate their stored energy in every switching cycle. Thus, conversion efficiency cannot be improved. Under the high-frequency operation, the lossy snubbers are no longer attractive. To solve the discussed problem, improved boost converters have been proposed.[7–14] Several types of lossless active and passive snubbers to improve the power losses of power semiconductor devices have been developed.[15–20] Passive lossless snubbers with simple structures need only passive switches and reactive components, which are usually operated at high efficiency. In this paper, we propose an improved boost converter with functions of adjustable output voltages and currents to reduce the high power losses and high temperatures of the power semiconductor devices, as shown in Fig. 1. The improved boost converter consists of two stages. The front stage is a boost converter with a passive lossless snubber and the rear stage is an analog control circuit with adjustable output voltages and currents.

The derivation of a passive lossless snubber is described in Sect. 2. The structure of the adjustable output voltage and current circuit is described in Sect. 3. The experimental results obtained from a prototype of the soft-switching boost converter with functions of adjustable output voltages and currents are presented in Sect. 4. Finally, the conclusions are given in Sect. 5.
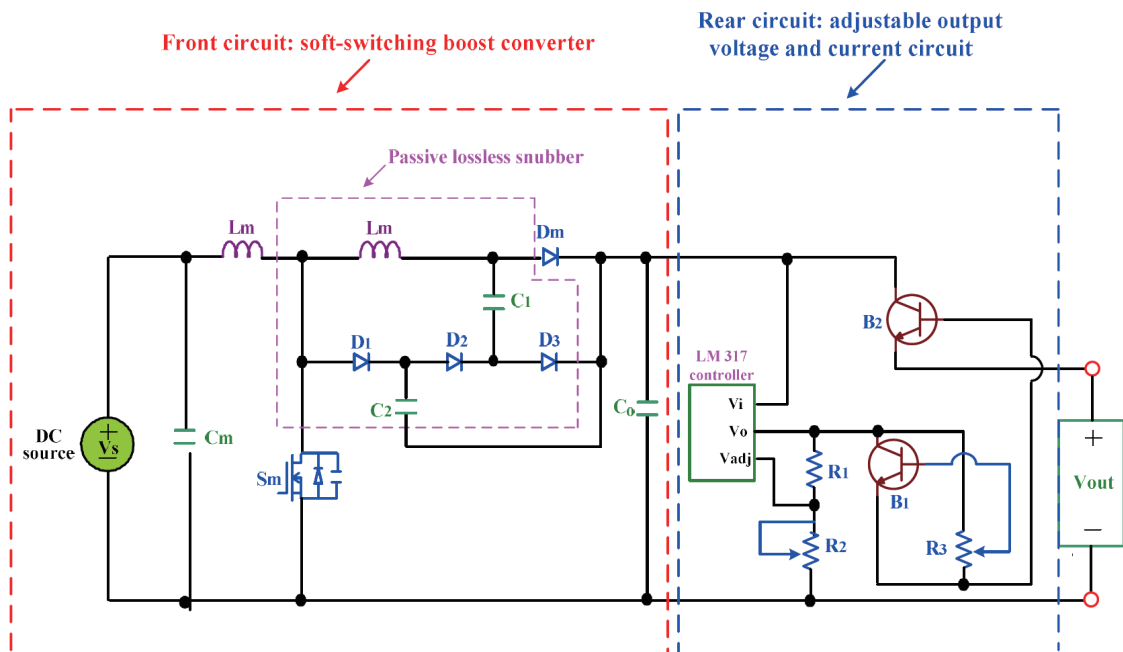

Fig. 1. (Color online) Topology of an improved boost converter with functions of adjustable output voltages and currents.

2.   Derivation of a Passive Lossless Snubber

The passive lossless snubber is applied by inserting passive components (diodes, inductors, and capacitors) to limit voltage and current spikes of the power semiconductor devices (power switches and power diodes). To illustrate the synthesis procedure, the conventional power converter combining two possible locations with a buffer capacitor (C_1 or C_2) and a bypass diode (D_1) is shown in Fig. 2. Both possible positions can realize the soft-switching of the conventional boost converter. The energy stored in the snubber capacitor (C_1 or C_2) must be transferred to the output before the switch (S_m) turn-off. For the power converter in Fig. 2, using an extra inductor (L_1) and two bypass diodes (D_2 and D_3) is an effective way to transfer the energy of a snubber capacitor, as shown in Fig. 3. During power switch (S_m) conduction, buffer capacitors (C_1 and C_2) and a snubber inductor (L_1) are operated in a resonating manner through the power switch
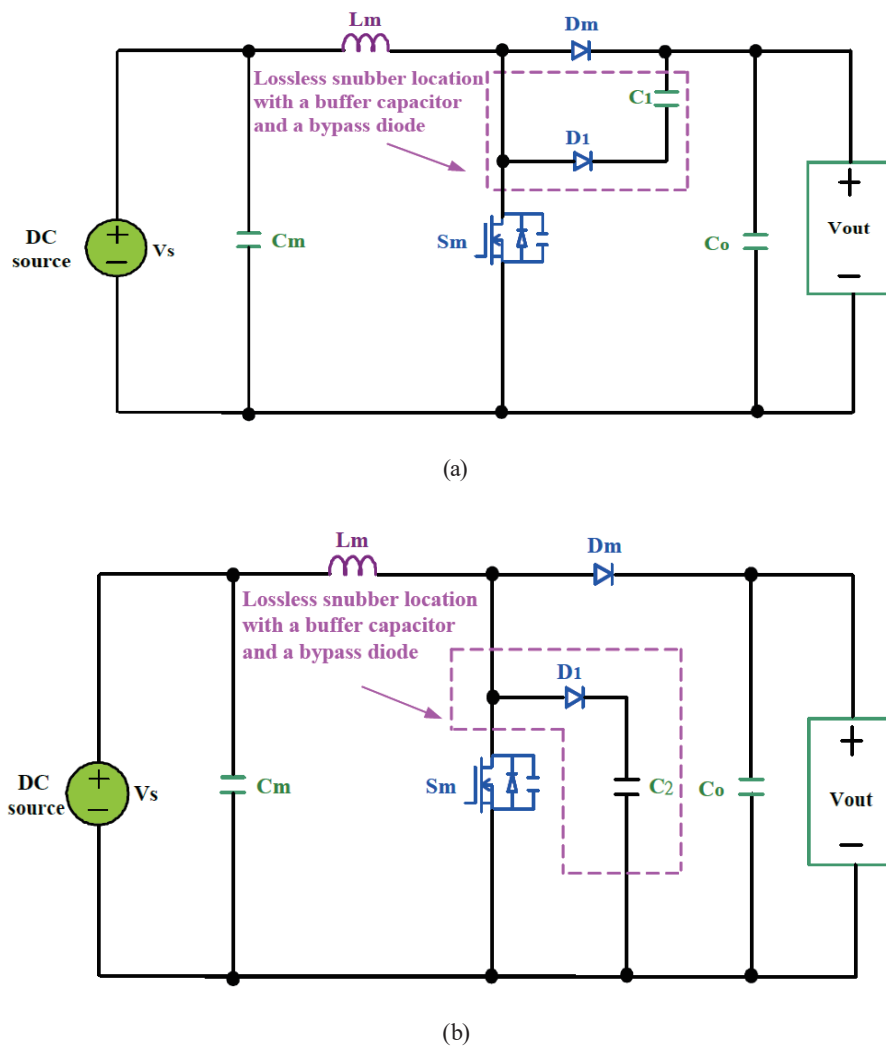

(a)

(b)

Fig. 2.   (Color online) Conventional boost converter combining two possible locations with a buffer capacitor (C_1 or C_2) and a bypass diode (D_1).
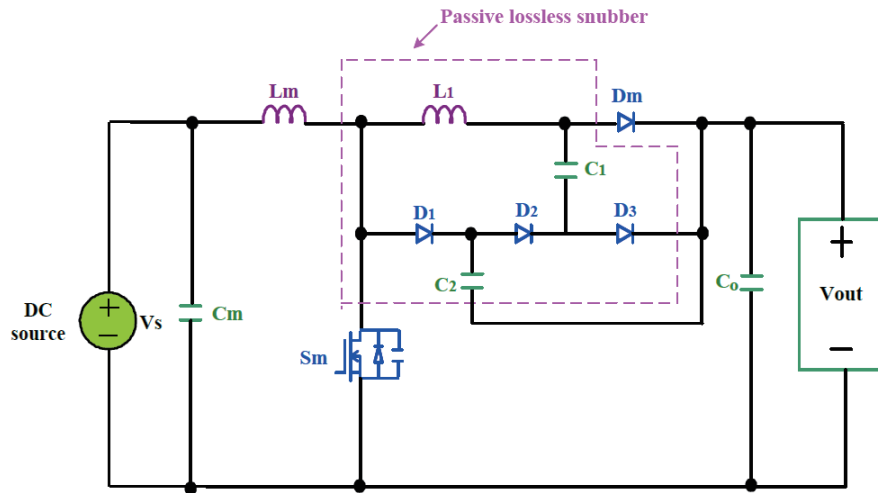
Fig. 3.   (Color online) Topology of conventional boost converter with a passive lossless snubber to implement soft-switching features.

(S_m) and bypass diode (D_2), and then the energy of the buffer capacitor (C_1) is transferred to the buffer capacitor (C_2). During power switch (S_m) turn-off, the buffer capacitor (C_2) and inductor (L_1) are operated in a resonating manner through bypass diodes (D_1 and D_2), and then the energy of the buffer capacitor (C_2) is transferred to the output. Therefore, the passive lossless buffer has a high conversion efficiency.

3.   Analysis of Adjustable Output Voltage and Current Circuit

In this section, we present the analysis of the adjustable output voltage and current circuit, as shown in Fig. 4. The circuit consists of an LM317 adjustable regulator, a constant resistor (R_1), two variable resistors (R_2 and R_3), and two transistors (B_1 and B_2). To describe its operational principles, the voltage and current characteristic curve of the transistors (B_1 and B_2) is shown in Fig. 5. The operational principles are analyzed as follows:

(1) When the variable resistor (R_2) is adjusted, the current I_{adj} is adjusted to set the voltage V_o of the LM317 adjustable regulator. The voltages of the V_o pin are calculated as shown in Eq. (1). According to Eq. (1), the terminal voltages of the V_{out} pin can be calculated as shown in Eq. (2). Therefore, the adjustable terminal voltages of V_{out} can be implemented.

$$V_o = 1.25\left(1 + \frac{R_2}{R_1}\right) + I_{adj}R_2, \tag{1}$$

and

$$V_{out} = V_o - V_{ce1} - V_{be2}, \tag{2}$$

where V_{ce1} is the collector-emitter voltage and V_{be} is the base-emitter voltage of a transistor.
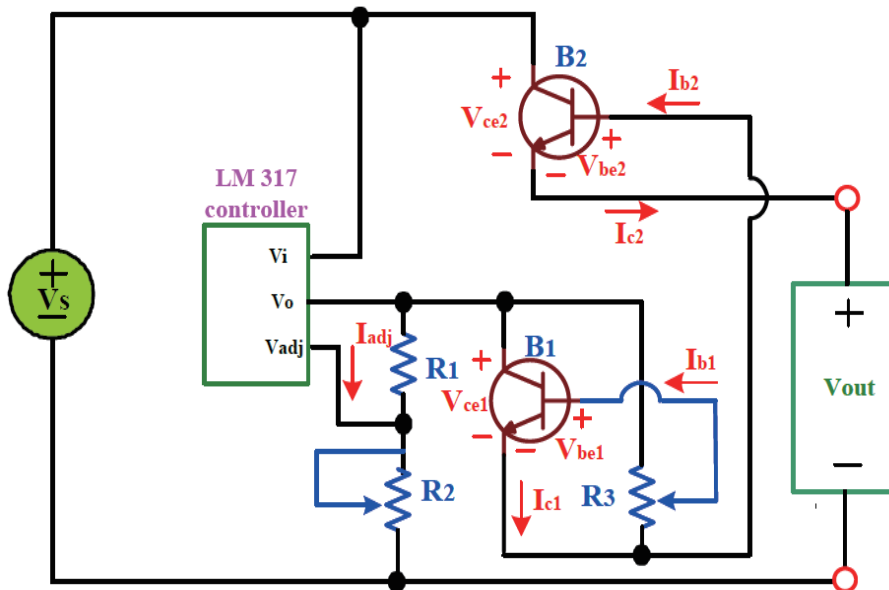
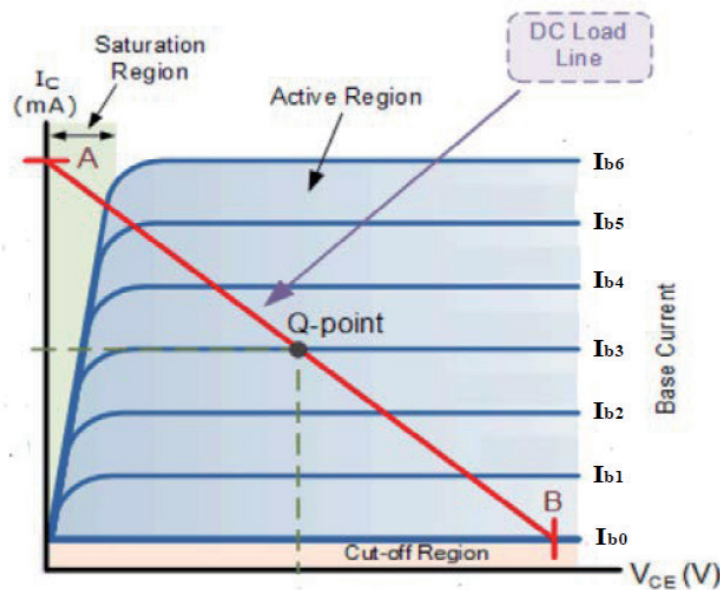Fig. 4.   (Color online) Adjustable output voltage and current circuit.

Fig. 5.   (Color online) Voltage and current characteristic curve of transistors.

(2) When the variable resistor (R_3) is adjusted, the base current I_{b1} of the transistor (B_1) is adjusted to control its collector-emitter voltage V_{ce1}. Thus, the linear collector current I_{c1} of the transistor (B_1) is obtained, as shown in Fig. 5. When the linear collector current I_{c1} of the transistor (B_1) is changed, the linear collector current I_{c2} of the transistor (B_2) is also changed. Therefore, adjustable terminal currents of V_{out} can be implemented.

4.   Experimental Results

To verify the performance of the soft-switching boost converter with functions of adjustable output voltages and currents, two stages of prototypes are built. In the front stage, the soft-switching boost converter with a passive lossless snubber is built. In the rear stage, the adjustable output voltage and current circuit is built.

The specifications of the soft-switching boost converter with a passive lossless snubber are shown as follows:
- input voltage: $V_s = 24$ V_{DC},
- output voltage: $V_o = 60$ V_{DC},
- maximum output current: $I_o = 1.2$ A,
- maximum output power: $P_{out} = 72$ W, and
- switching frequency of active switches: $f = 50$ kHz.

The specifications of the adjustable output voltage and current circuit are shown as follows:
- input voltage: $V_{in} = 60$ V_{DC},
- adjustable output voltage: $V_{out} = 0–60$ V_{DC},
- maximum output current: $I_o = 1$ A, and
- maximum output power: $P_{out} = 60$ W.

In this section, the experimental results of the conventional and improved boost converters are compared. Figures 6 and 7 respectively indicate the current and voltage waveforms of the power switch (S_m) and power diode (D_m) of the conventional and improved boost converters. It can be seen that the improved boost converter has lower power losses at the turned-on and turned-off switching transitions. Figure 8 shows the temperature waveforms of the power switch (S_m) of the conventional and improved boost converters. It can be seen that the power switch (S_m) of the improved boost converter has lower temperatures. Figures 9–12 show the output voltages and currents of the adjustable output voltage and current circuit operated at output voltages of 12, 24, 36 and 48 V, respectively, and output currents of 0.5 and 1 A. It can also be seen that the functions of the adjustable output voltages and currents can be easily implemented by the adjustable output voltage and current circuit.
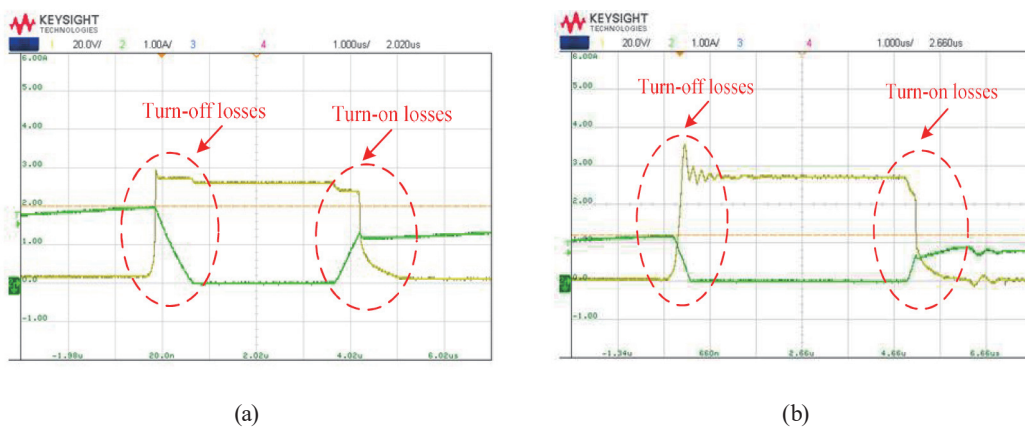

(a)   (b)

Fig. 6.   (Color online) Measured voltage and current waveforms of power switch (S_m) operated at turn-on and turn-off switching transitions: (a) conventional and (b) improved boost converters.
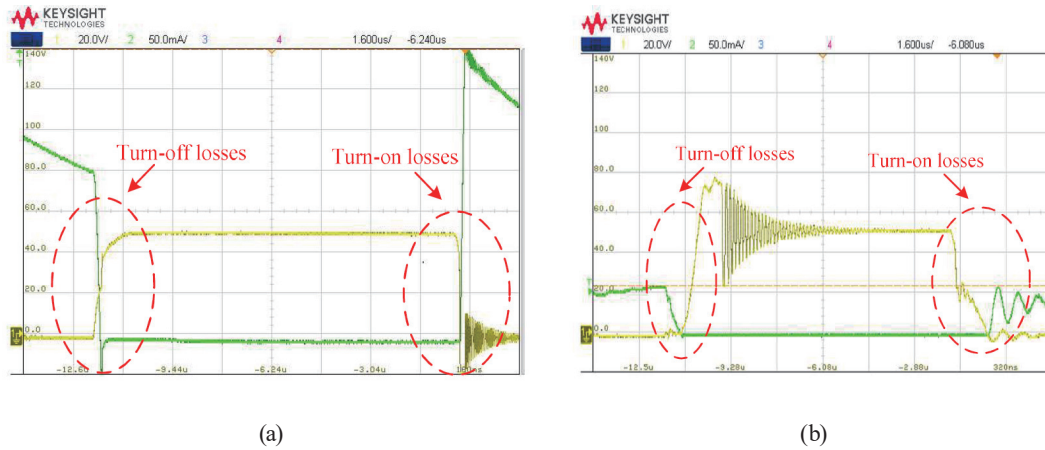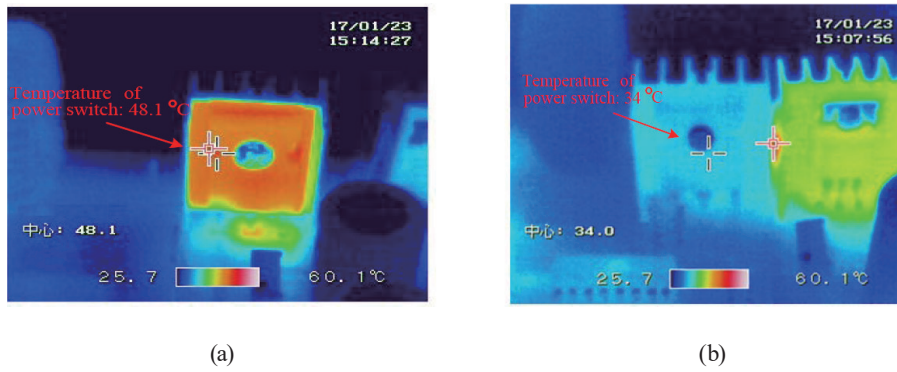
(a)   (b)

Fig. 7.   (Color online) Measured voltage and current waveforms of power diode (D_m) operated at turn-on and turn-off switching transitions: (a) conventional and (b) improved boost converters.

(a)   (b)

Fig. 8.   (Color online) Measured temperatures of power switch (S_m) operated under full-load condition: (a) conventional and (b) improved boost converters.

(a)
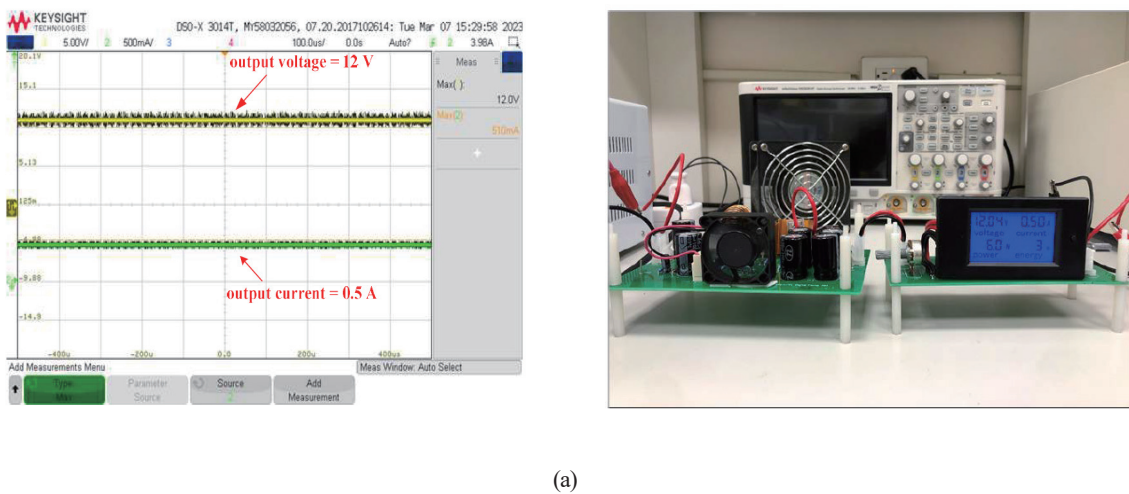
Fig. 9.   (Color online) Measured adjustable output voltages and currents: (a) 12 V and 0.5 A, and (b) 12 V and 1 A.
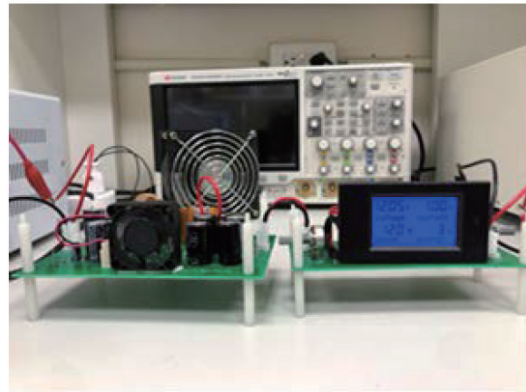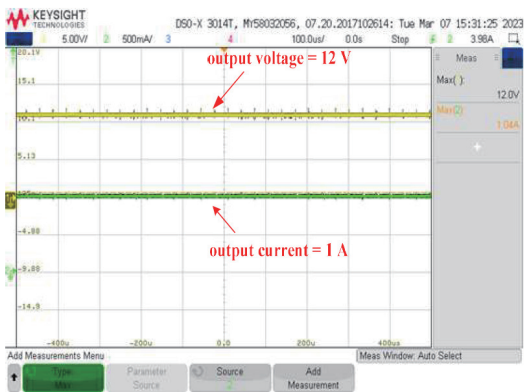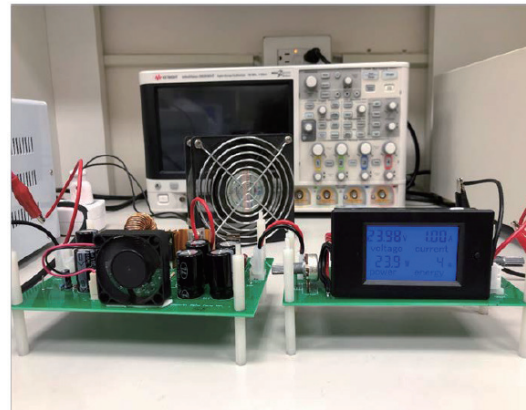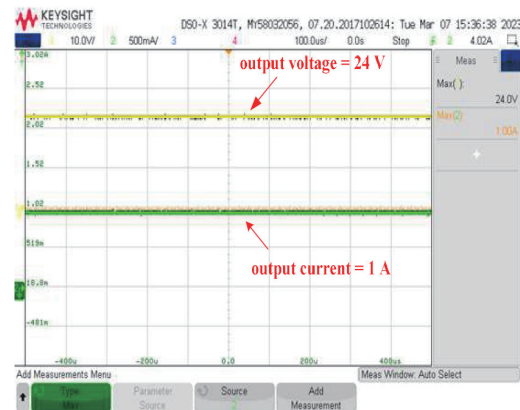
(b)

Fig. 9.   (Continued) (Color online) Measured adjustable output voltages and currents: (a) 12 V and 0.5 A, and (b) 12 V and 1 A.
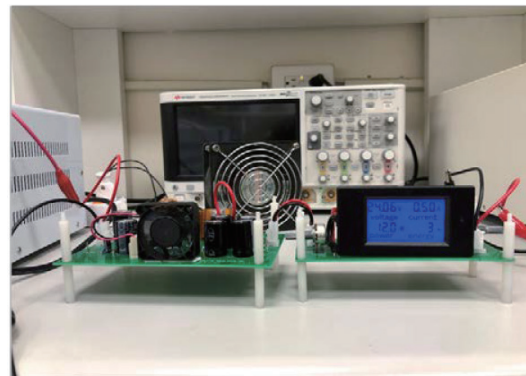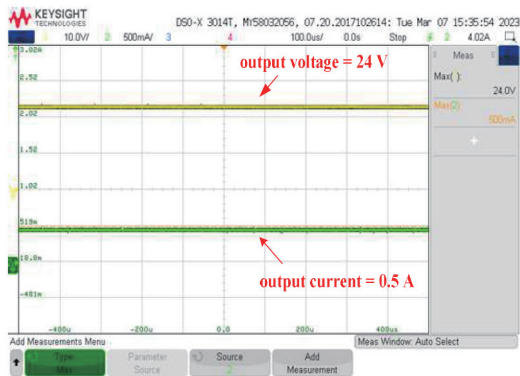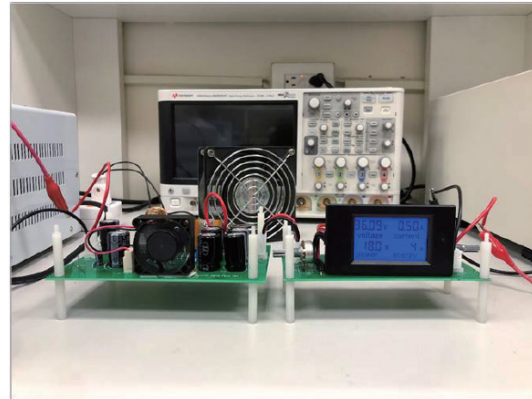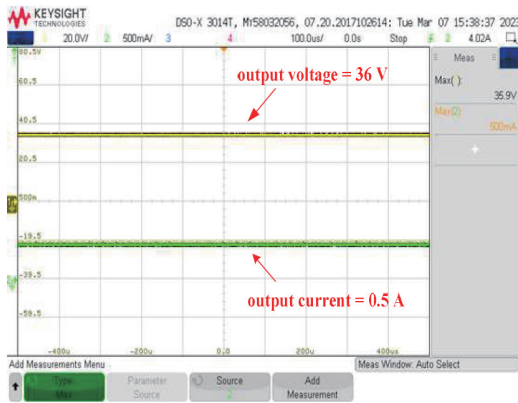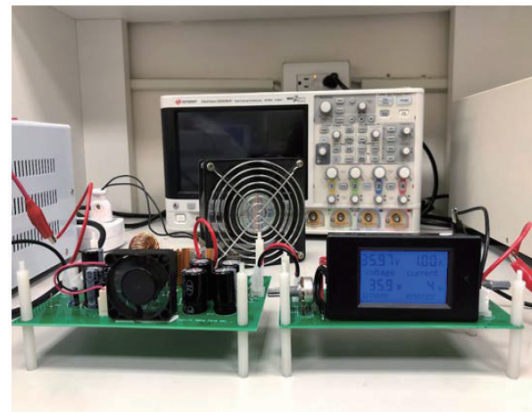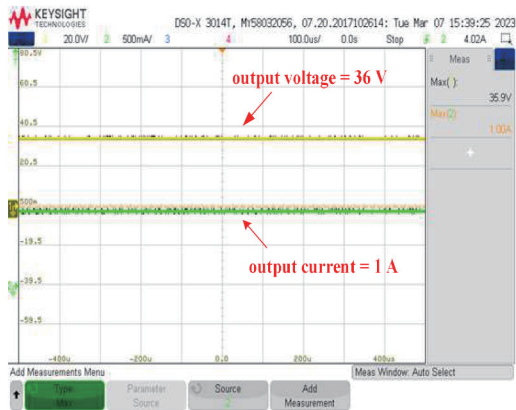

(a)

(b)

Fig. 10.   (Color online) Measured adjustable output voltages and currents: (a) 24 V and 0.5 A, and (b) 24 V and 1 A.
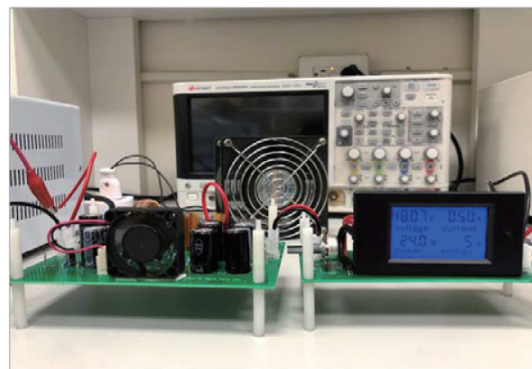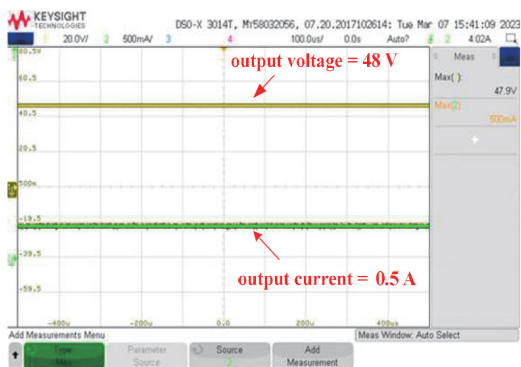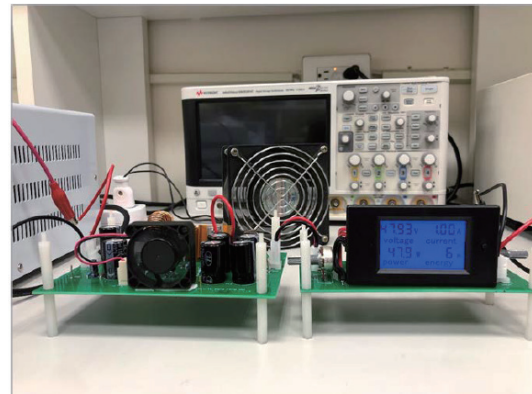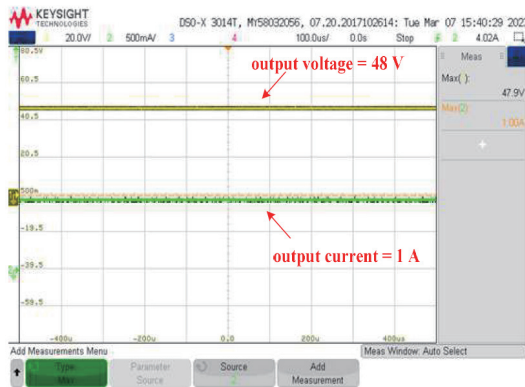
(a)

(b)

Fig. 11.   (Color online) Measured adjustable output voltages and currents: (a) 36 V and 0.5 A, and (b) 36 V and 1 A.

(a)

Fig. 12.   (Color online) Measured adjustable output voltages and currents: (a) 48 V and 0.5 A, and (b) 48 V and 1 A.

(b)

Fig. 12.   (Continued) (Color online) Measured adjustable output voltages and currents: (a) 48 V and 0.5 A, and (b) 48 V and 1 A.

5.   Conclusions

In this paper, we proposed an improved boost converter with functions of adjustable output voltages and currents. The performance characteristics of the conventional and improved boost converters were compared. From the measured voltage, current, and temperature waveforms of the conventional and improved boost converters, it was seen that the improved boost converter has lower power losses and temperatures. This is because the power switch (S_m) and power diode (D_m) of the improved boost converter use a passive lossless snubber to implement soft-switching features. Additionally, the output voltages and currents can be easily adjusted using the proposed adjustable circuit. From all the measurement results, it was proved that the improved boost converter with functions of adjustable output voltages and currents has lower switching losses and temperatures.

Author Contributions

Cheng-Tao Tsai designed the circuit and wrote the paper, and Feng-Wei Peng developed the measurement circuit.

Conflicts of Interest

The authors declare no conflicts of interest.

References

1   J. C. Su, C. T. Tsai, and T. C. Liang: Sens. Mater. **34** (2022) 1697. https://doi.org/10.18494/SAM3816
2   C. T. Tsai, J. C. Su, and S. R. Wei: Sens. Mater. **31** (2019) 327. https://doi.org/10.18494/SAM.2019.2086
3   K. J. Boelter and J. H. Davidson: Aero. Sci. Techno. **27** (1997) 689. https://doi.org/10.1080/02786829708965505
4   K. W. E. Cheng, B. P. Divakar, H. Wu, K. Ding, and H. F. Ho: IEEE Trans. Vehicular Technology. **60** (2010) 76. https://doi.org/10.1109/TVT.2010.2089647

5   M. Ceraolo and G. Pede: IEEE Trans. Vehicular Technology. **50** (2001) 109. https://doi.org/10.1109/25.917893

6   A. Ajami, H. Ardi, and A. Farakhor: IEEE Trans. Power Electron. **30** (2015) 4255. https://doi.org/10.1109/TPEL.2014.2360495

7   I. Batarseh: IEEE Trans. Power Electron. **9** (1994) 64. https://doi.org/10.1109/63.285495

8   R. L. Steigerwald: IEEE Trans. Power Electron. **3** (1988) 174. https://doi.org/10.1109/63.4347

9   C. J. Tseng and C. L. Chen: IEEE Trans. Ind. Electron. **45** (1998) 593. https://doi.org/10.1109/41.704887

10 L. Liu, J. Guo, J. Li, and L. Sheng: J. Elect. **48** (2000) 81. https://doi.org/10.1016/S0304-3886(99)00049-2

11 T. F. Wu, Y. D. Chang, C. H. Chang, and J. G. Yang: IEEE Trans. Power Electron. **27** (2012) 1108. https://doi.org/ 10.1109/TPEL.2011.2126024

12 H. Wang, H. S. Chung, and A. Ioinovici: IEEE Trans. Power Electron. **27** (2012) 2242. https://doi.org/10.1109/TPEL.2011. 2173588

13 A. Ajami, H. Ardi, and A. Farakhor: IEEE Trans. Power Electron. **30** (2015) 4255. https://doi.org/10.1109/TPEL.2014.2360495

14 T. F. Wu, Y. D. Chang, C. H. Chang, H. X. Lee, K.-Y. Lee, and J.-G. Yang: 2009 Inter. Conf. Power Electron. and Drive Syst. (PEDS, 2009) 187. https://doi.org/10.1109/PEDS.2009.5385795

15 S. Y. Tseng and C. T. Tsai: Int. J. Photoenergy. **2012** (2012) 1. https://doi.org/10.1155/2012/936843

16 W. Hao, J. Gong, X. Zhao, C. S. Yeh, and J. S. Lai: IEEJ Trans. Power Electron. **34** (2019) 11952. https://doi.org/ 10.1109/TPEL.2019.2909426

17 T. F. Wu, Y. D. Chang, C. H. Chang and J. G. Yang: IEEE Trans. Power Electron. **27** (2012) 1108. https://doi.org/ 10.1109/TPEL.2011.2126024

18 Y. M. Chen, S. Y. Tseng, C. T. Tsai and T. F. Wu: IEEE Trans. Aero. Electron. Syst. **40** (2004) 954. https://doi.org/ 10.1109/TAES.2004.1337467

19 L. M. Redondo: IEEE Trans. Plasma Sci. **38** (2010) 2725. https://doi.org/10.1109/TPS.2010.2050495

20 J. Zhang, D. D.-C. Lu, and T. Sun: IEEE Trans. Ind. Electron. **57** (2010) 1041. https://doi.org/10.1109/TIE.2009.2028336